Contents lists available at ScienceDirect

Journal of Alloys and Compounds

journal homepage: www.elsevier.com

UNCORRECTED PROOF

Diffusion barrier property of electroless Ni-W-P coating in high temperature Zn-5Al/Cu solder interconnects

Li Liu[a, b], Zhiwen Chen[a d,?], Zhaoxia Zhou[c], Guang Chen[b, d], Fengshun Wu[d], Changqing Liu[b, *]

[a] *School of Materials Science and Engineering, Wuhan University of Technology, Wuhan, 430070, China*
[b] *Wolfson School of Mechanical, Electrical and Manufacturing Engineering, Loughborough University, Loughborough, Leicestershire, LE11 3TU, UK*
[c] *Loughborough Materials Characterisation Centre, Loughborough University, Loughborough, Leicestershire, LE11 3TU, UK*
[d] *School of Materials Science and Engineering, Huazhong University of Science and Technology, Wuhan, 430074, China*

ARTICLE INFO

Article history:
Received 14 February 2017
Accepted 11 June 2017
Available online xxx

Keywords:
Zn-5Al solder
Electroless Ni-W-P coating
Diffusion barrier
Interfacial reaction
Kirkendall voids

ABSTRACT

The operating temperature of high-temperature electronics can significantly promote the growth of intermetallic compounds (IMCs) at solder/substrate interfaces, particularly for low-cost Zn-based solders because of the rapid rate of reaction of Zn with Cu. Thus, a reliable and robust diffusion barrier is indispensable for suppressing the reactions between solder and substrate. In this work, a ternary Ni-W-P alloy was prepared via electroless plating. Its diffusion barrier property was evaluated by comparing the microstructures of IMC layers in Zn-5Al/Ni-W-P/Cu and Zn-5Al/Cu interconnects after liquid-solid reaction for prolonged durations. When the reaction lasted for 30 min, the thickness of the Al_3Ni_2 produced in the Zn-5Al/Ni-W-P/Cu solder interconnects was only 2.15 μm, whereas the thickness of the interfacial layer of Cu-Zn IMCs ($CuZn_4$, Cu_5Zn_8 and CuZn) at the Zn-5Al/Cu interface was 94 μm. Because of the unbalanced growth of the IMCs in the Zn-5Al/Cu interconnects, notable numbers of Kirkendall voids were identified at the $CuZn_4$/Cu_5Zn_8, Cu_5Zn_8/CuZn and CuZn/Cu interfaces after prolonged liquid-solid reaction. By contrast, the Al_3Ni_2 layer in the Zn-5Al/Ni-W-P/Cu solder joints remained intact, showing the potential to effectively enhance the mechanical reliability of electronic devices.

© 2017.

1. Introduction

High-lead solders (Pb content: 85–97 wt.%) are commonly applied in high-temperature electronics (HTE), including devices for use in aircraft, automotive, space and drilling applications [1,2]. However, due to health and environmental concerns, the development of high-temperature lead-free solders to replace lead solders is of vital importance. Recently, considerable research has been conducted on various high-temperature alternatives, including Au-rich, Bi-Ag, and Zn-based solders as well as nano-silver paste. Unfortunately, certain notable drawbacks have limited their applications, such as the high cost of Au-rich solder [3], the low wettability and brittleness of Bi-Ag solder [4], and the high cost and porosity of nano-silver assemblies [5,6]. Among these alternatives, Zn-based solder is a potential lead-free candidate by virtue of its low cost, high melting point, and good thermal and electrical conductivity, and thus, this potential solder material deserves further investigation [7,8].

However, Zn-based solders actively react with Cu substrates to produce excessive Cu-Zn intermetallic compounds (IMCs), particularly at elevated temperatures. This makes solder joints brittle and prone to fracture [9]. To solve this challenge, diffusion barriers can be utilised to hinder the interfacial reactions in Zn-based solder joints. In industry, electroless Ni-P coatings have been widely employed as diffusion barriers in conventional electronics. Unfortunately, this alloy is not suitable for HTE because of its low crystallisation temperature and weak thermal stability as well as the voids that form in a crystalline Ni_3P layer [10–12]. Therefore, a reliable and robust diffusion barrier that functions stably is critically required for high-temperature solder joints, especially for Zn-5Al solder, a typical high-temperature solder. Previous works have reported that the incorporation of W can significantly retard the crystallisation of electroless Ni-P alloys [13–15]. Moreover, a few researchers have studied the reactions of Ni-W-P coatings with Sn-Bi or Sn-3.5Ag solders, drawing the conclusion that the interfacial reactions with a Ni-W-P interlayer are clearly slower than those with a Ni-P interlayer [15–17]. However, these solders are generally applied in a relatively low-temperature regime (peak reflow temperature < 220 °C).

To date, the interfacial reactions between electroless Ni-W-P layers and high-temperature solders during reflow has seldom been reported. In this work, the effects of electroless Ni-W-P coatings on inhibiting the interfacial reactions in Zn-5Al solder interconnects were investigated in comparison with a bare Cu substrate. Attention was directed towards the reduction of the growth rates of interfacial IMC layers and the prevention of Kirkendall void formation at the solder/substrate interface during liquid-solid reaction after the application of an electroless Ni-W-P coating. The morphological evolution of the IMCs at these interfaces was also investigated.

* Corresponding author.
Email address: C.Liu@lboro.ac.uk (C. Liu)

http://dx.doi.org/10.1016/j.jallcom.2017.06.122
0925-8388/© 2017.

2. Experimental procedures

2.1. Electroless Ni-W-P plating

An electroless Ni-W-P ternary alloy was produced on polycrystalline copper substrates. Prior to electroless plating, a pre-polished Cu sheet (99.9% purity, 1 mm thickness) was cut into square pieces (20 × 20 mm) and then ultrasonically cleaned with acetone followed by 50 vol.% HCl acid to remove oil and oxidation, respectively. Next, these copper substrates were immersed in a plating bath, and an aluminium wire was subsequently attached to the copper surface to initiate deposition. The wire was then removed after the formation of an initial thin Ni-W-P layer. The plating solution was an alkaline bath consisting of deionised water and sodium tungstate (7 g/L), nickel sulphate (35 g/L), sodium hypophosphite (12 g/L) and sodium acetate (40 g/L). The plating temperature was 88 ± 2 °C, and the plating time was 30 min. After deposition, all substrates were cleaned and dried for the preparation of the solder interconnects.

2.2. Preparation of Zn-5Al solder interconnects

Prior to reflow, Zn-5Al solder pellets (weight: approximately 0.15 g, melting point: 382 °C) were placed on Ni-W-P-plated Cu substrates and bare Cu substrates for comparison. The reflow was conducted on a hotplate attached to a temperature control unit to perform a reflow profile as shown in Fig. 1. A K-type thermal couple that measured real-time temperature of the samples validated the consistency with the pre-set temperature profile. The durations of reaction between the molten Zn-5Al solders and the solid Cu substrates ranged from 1 to 30 min.

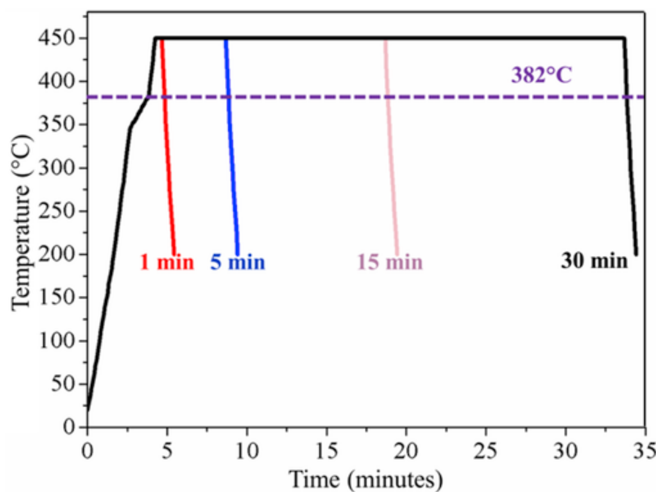

Fig. 1. Reflow temperature profiles of the Zn-5Al solder interconnects.

2.3. Morphological and microstructural observations

After reflow, some specimens were cold mounted, ground and finally polished using colloidal silica to reveal their cross-sectional microstructures. The microstructures of the interfacial IMCs that formed at the Zn-5Al/Cu and Zn-5Al/Ni-W-P/Cu interfaces under the same reflow conditions were investigated using scanning electron microscopy (SEM, Zeiss 1530VP) combined with energy-dispersive X-ray spectroscopy (EDS). The thicknesses of the Ni-W-P coatings and IMC layers were also measured using ImageJ software. Meanwhile, the top-view morphologies of the IMCs formed in the Zn-5Al/Ni-W-P solder interconnects were examined by etching the Zn-5Al solders with a dilute NaOH solution (20 g/L).

3. Results and discussion

3.1. As-deposited electroless Ni-W-P coating

The as-deposited Ni-W-P coating consisted of 7–8 wt.% P and 18–19 wt.% W, according to the EDX analysis. The surface morphology and cross section of this Ni-W-P coating are shown in Fig. 2. Its surface exhibited a typical cauliflower-like morphology with smooth nodules of uneven size (size range: 0.5–1.5 μm). No visible defects and pores were observed on its surface. As shown in Fig. 2 b), the thickness of the Ni-W-P coating was approximately 2 μm. Overall, this coating was free of cracks, compact and adherent, showing good properties as a barrier layer. It was firmly adhered to the Cu substrate, as no visible pores could be seen at the interface.

3.2. Evolution of IMC morphologies during liquid-solid reaction

The cross-sectional microstructures and corresponding topographies of the interfacial IMCs in Zn-5Al/Ni-W-P/Cu solder interconnects are shown in Fig. 3. According to their cross-sectional microstructures in Fig. 3a), c), e) and g), only one thin IMC layer formed at the Zn-5Al/Ni-W-P interfaces, with a thickness that increased from 0.5 to 2.15 μm as the liquid-solid reaction duration increased from 1 to 30 min. To precisely identify this IMC layer, elemental analysis was performed on the Zn-5Al/Ni-W-P solder interconnects subjected to the longest reaction time (30 min), and the composition was identified as Al_3Ni_2, as presented in Fig. 4.

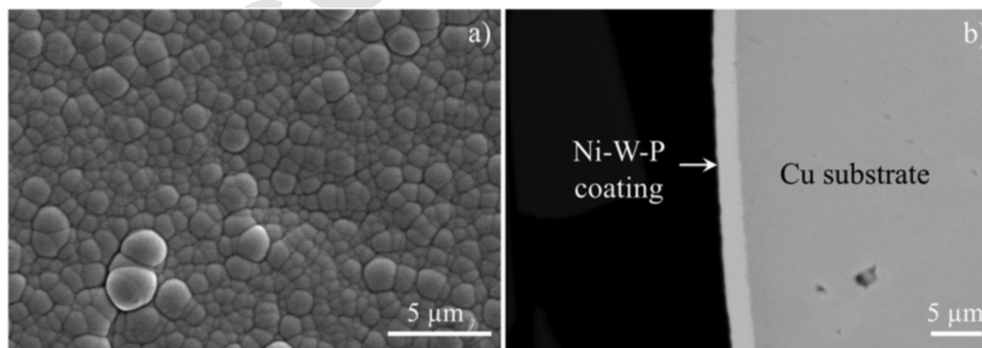

Fig. 2. Micrographs of an as-deposited Ni-W-P coating: a) surface morphology and b) cross-sectional morphology.

UNCORRECTED PROOF

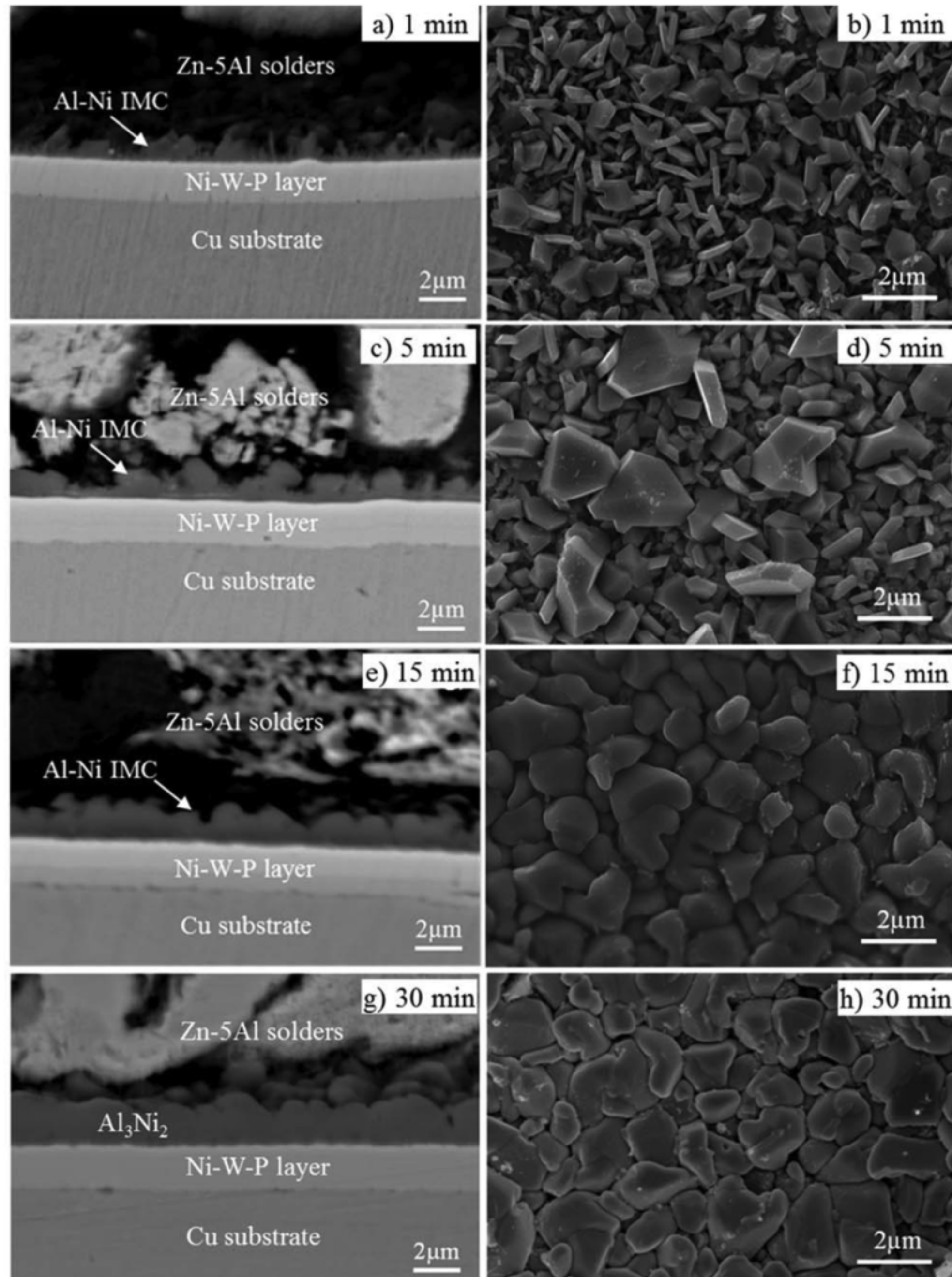

Fig. 3. Cross-sectional views (a, b, c and d) and top views (e, f, g and h) of Zn-5Al/Ni-W-P interfaces after reflow at 450 °C for various reaction times: (a and d) 1 min, (b and e) 5 min, (c and f) 15 min, and (g and h) 30 min.

Regarding the topography of the Al_3Ni_2, after 1 min of reaction, the generated Al_3Ni_2 (0.5 μm in thickness) exhibited prism-like or plate-like shapes, as shown in Fig. 3 b). As the reaction time increased to 5 min, the average thickness of the Al_3Ni_2 layer grew to approximately 0.9 μm. The plate-like IMCs transformed into rod-like shapes, whereas the prism-like IMCs continuously grew to a larger size of approximately 2 μm (Fig. 3 d). After liquid-solid reaction for 15 min, some of the larger Al_3Ni_2 grains (size: ~2 μm) continued to grow into round scalloped shapes by merging with adjacent smaller Al_3Ni_2 grains (size: ~0.2 μm), resulting in a continuous Al_3Ni_2 layer, as illustrated in Fig. 3 e). The size of these scalloped IMCs ranged from 1 to 2.1 μm. Finally, after 30 min of reaction, faceted scallops with a polygonal shape were observed, with a slightly increased grain size (up to 2.5 μm) as shown in Fig. 3 h). Overall, the shapes of the Al_3Ni_2 grains transformed from initial prism-like or plate-like shapes into rod-like shapes and subsequently grew into scallop shapes.

From the elemental mapping results for this solder interface after 30 min of reaction (see Fig. 4), it is clear that Ni atoms in the Ni-W-P coating diffused out and reacted with Al atoms from the Zn-5Al solder to form Al_3Ni_2. By contrast, the signals from Zn and Cu were observed to terminate at the Zn-5Al/Al_3Ni_2 and Ni-W-P/Cu interfaces, respectively. This indicates that Zn and Cu atoms did not diffuse through the Ni-W-P interlayer, thereby demonstrating its excellent diffusion barrier property for eliminating the interdiffusion of

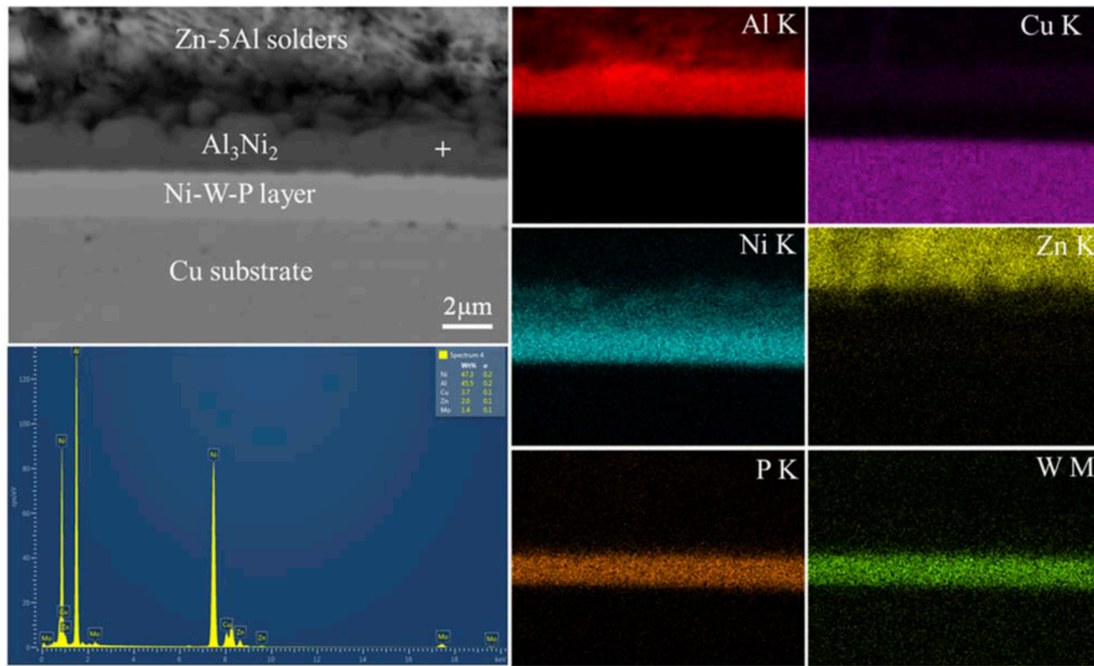

Fig. 4. Elemental mapping and pointing analysis of a Zn-5Al/Ni-W-P interface after 30 min of liquid-solid reaction at 450 °C.

Zn and Cu. It has been reported that in Zn-4Al/Ni solder interconnects, Al_3Ni_2 grains peel from the Ni substrate and disperse into the solder matrix to form a thick zone after 5 min of liquid-solid reaction at 450 °C [18]. However, no spalling of the Al_3Ni_2 occurred in the Zn-5Al/Ni-W-P system, even after liquid-solid reaction for up to 30 min at 450 °C. This observation thus additionally confirms the excellent diffusion barrier property of an electroless Ni-W-P interlayer compared with a bare Ni substrate.

For Zn-5Al solder interconnects without a Ni-W-P interlayer, cross-sectional micrographs of the IMCs formed after liquid-solid reaction at 450 °C for up to 30 min are presented in Fig. 5. The compositions of these IMC phases are shown in Table 1. The thickness of the interfacial IMCs at the Zn-5Al/Cu interface (94 μm, 30 min of reaction) was much higher than it was at the Zn-5Al/Ni-W-P interface (2.15 μm, 30 min of reaction). Such a high IMC thickness could cause problems in interfacial integrity due to the brittle nature of IMCs and their mismatches with the physical properties (e.g., elastic

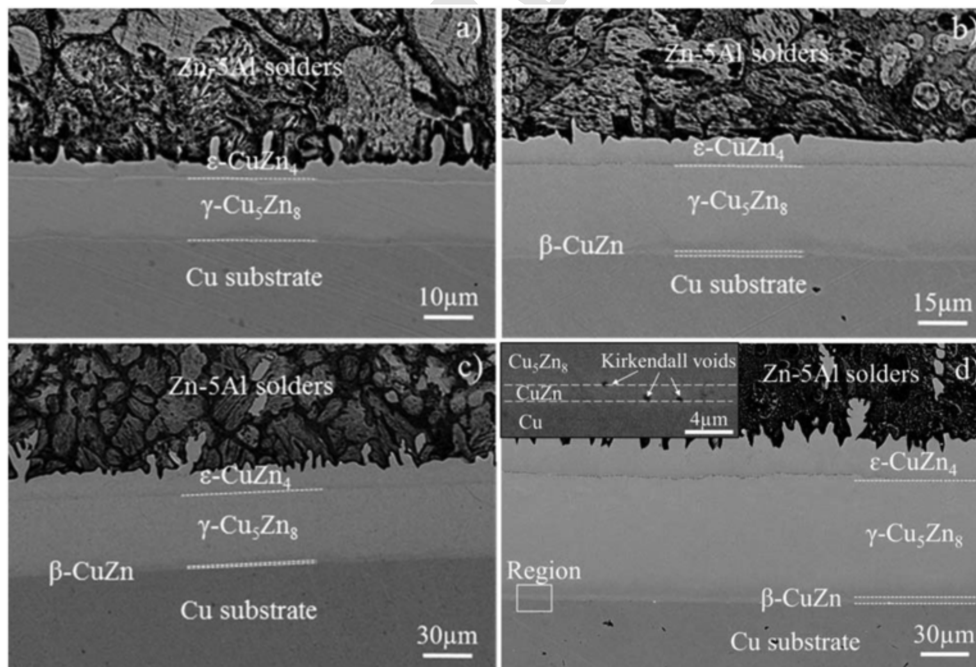

Fig. 5. Backscattered SEM images showing the IMCs formed at Zn-5Al/Cu interfaces after liquid-solid reaction for a) 1 min, b) 5 min, c) 15 min, and d) 30 min.

Table 1
Results of a quantitative EDX analysis of the IMCs formed at a Zn-5Al/Cu interface.

Position	Cu composition (at.%)	Zn composition (at.%)	Corresponding IMC
Upper layer	20.3	79.7	ε-$CuZn_4$
Medium layer	39.1	60.9	γ-Cu_5Zn_8
Lower layer	52.3	47.7	β-CuZn

moduli and coefficients of thermal expansion) of the solder and substrate [19–21].

After 1 min of reaction, the upper layer adjacent to the Zn-5Al solder was a dendritic ε-$CuZn_4$ layer (~4 μm), whereas an interlayer of γ-Cu_5Zn_8 (~12.5 μm) had formed between the $CuZn_4$ and the Cu substrate. The activation energies for the formation of $CuZn_4$ and Cu_5Zn_8 have been reported to be 29.54 and 42.38 kJ/mol, respectively [22]. Therefore, it can be inferred that $CuZn_4$ was likely the first IMC to be produced at the Zn/Cu interface, followed by the formation of Cu_5Zn_8. After 5 min of liquid-solid reaction, the thicknesses of the $CuZn_4$ and Cu_5Zn_8 had grown to 8 μm and 27 μm, respectively. A thin layer of β-CuZn (thickness: ~1 μm) emerged between the $CuZn_4$ and the Cu substrate, as shown in Fig. 5 b), consistent with the results of a previous study [23]. In addition, numerous Kirkendall voids were also found at this $CuZn_4$/Cu_5Zn_8 interface, which is in accordance with previous work on the Zn-Sn-Cu-Bi solder system [24]. With the prolongation of the reflow duration with molten solder, the thickness of the Cu-Zn IMCs continued to increase, to approximately 65 μm after 15 min of reaction and 94 μm after 30 min of reaction.

Notably, a few Kirkendall voids emerged near the CuZn interlayer (see the enlarged region in Fig. 5d)) in the Zn-5Al/Cu solder interconnects after 30 min of reaction. This phenomenon has not previously been reported in Zn-based solder joints, but it is similar to the observations of voids in Cu_3Sn layers in aged Sn/Cu solder joints [12,25,26]. The formation of these nano-sized voids can be attributed to the difference between the intrinsic diffusivities of Cu and Zn. The CuZn/Cu and Cu_5Zn_8/CuZn interfaces served as locations for the agglomeration of defects into nano-/micro-voids (Kirkendall voids) near the interfaces. Such voids can seriously degrade the reliability of solder joints by acting as crack initiation regions when subjected to external loads [27]. Moreover, during service, these voids are likely to propagate with the growth of CuZn and aggregate to larger sizes, resulting in significant mechanical and electrical degradation of the solder joints [28,29].

3.3. IMC growth kinetics during liquid-solid reactions

Fig. 6 shows the parabolic relationships between the thicknesses of all IMCs and the liquid-solid reaction durations for Zn-5Al/Cu and Zn-5Al/Ni-W-P interfaces reacted at 450 °C for 1, 5, 15 and 30 min. The thickness of the total Cu-Zn IMC layer at the Zn-5Al/Cu interface grew significantly, from approximately 17 μm (after 1 min of reaction) to 94 μm (after 30 min of reaction), as shown in Fig. 6 a), whereas the thickness of the Al_3Ni_2 at the Zn-5Al/Ni-W-P interface grew only from 0.5 μm (after 1 min of reaction) to 2.15 μm (after 30 min of reaction). Fig. 6 b) shows the individual Cu-Zn IMC thicknesses; the γ-Cu_5Zn_8 interlayer was the thickest among them, and the $CuZn_4$ was the layer of intermediate thickness. Previous studies have reported that the rapid growth of Cu_5Zn_8 is a result of the high diffusion rates of Cu and Zn atoms in the $CuZn_4$ phase [22,30]. By contrast, the growth rate of CuZn was the slowest among the three Cu-Zn IMCs, with this layer reaching a maximum thickness of 2.5 μm after

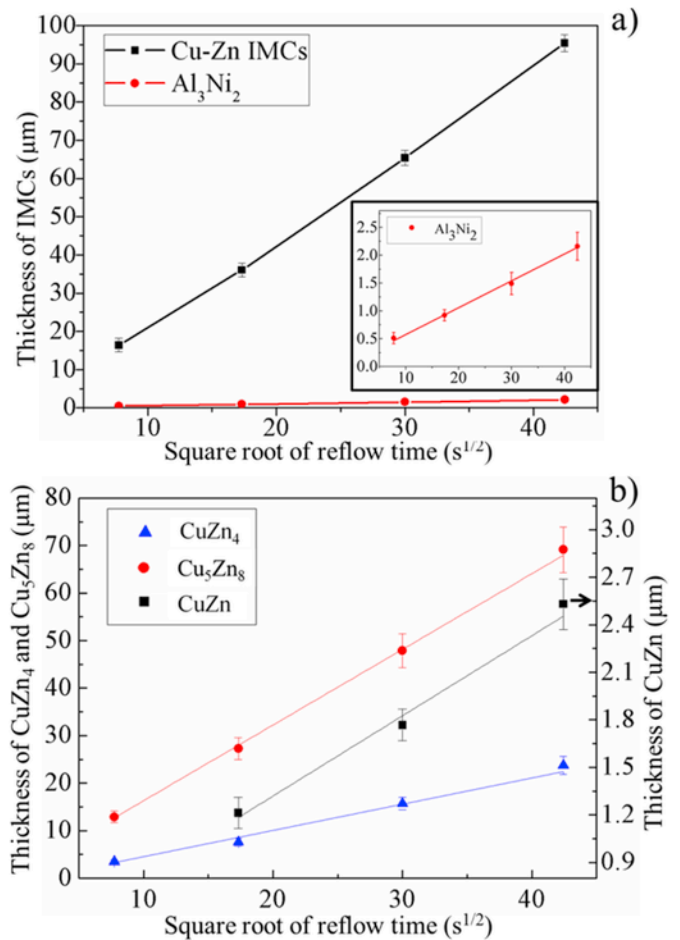

Fig. 6. Thicknesses of the Zn-Cu IMCs formed after liquid-solid reaction at 450 °C for 1, 5, 15 and 30 min at a) Zn-5Al/Cu interfaces and b) Zn-5Al/Ni-W-P interfaces.

30 min of reaction. However, at the Zn-5Al/Ni-W-P solder interface after 30 min of reaction, the growth rate of Al_3Ni_2 was even slower than that of CuZn, which was the slowest IMC to form at the Zn-5Al/Cu solder interface.

Generally, it was clearly observed that the IMC thickness (d) increased linearly with the square root of t. This linear relationship indicates that the growth mechanisms of all IMCs were diffusion-controlled, consistent with the following parabolic law:

$$d = k\sqrt{t} \tag{1}$$

where d is the thickness of the IMC layer, t is the liquid-solid reaction duration, and k is the growth rate coefficient for the IMC of interest, which can be calculated for each IMC from the slope of the corresponding fit line in Fig. 6.

In this way, the experimental values of k for the different interfacial IMCs that form in Zn-Al solder interconnects under harsh conditions were calculated and are listed in Table 2.

For the Zn-5Al solder interconnects with Ni-W-P coatings, the growth rate coefficient (k) of the Al_3Ni_2 layer was 4.9×10^{-2} μm/$s^{1/2}$ because of the slow reaction rate between the molten Zn-5Al solder and the Ni-W-P coating. During the initial liquid-solid reaction (1 min), a good metallurgical and electrical bond was achieved through a thin Al_3Ni_2 layer with a reasonable thickness (~0.5 μm).

Table 2
Comparison of the formation and growth of IMCs at Zn-5Al/Ni-W-P and Zn-5Al/Cu interconnects during liquid-solid reactions.

Solder interconnect	IMC	k ($\mu m/s^{1/2}$)	Reflow temperature (°C)
Zn-5Al/Ni-W-P	Al_3Ni_2	4.90×10^{-2}	450
Zn-5Al/Cu	Cu-Zn IMCs	2.180	450
	ε-$CuZn_4$	5.506×10^{-1}	450
	γ-Cu_5Zn_8	1.573	450
	β-CuZn	5.607×10^{-2}	450

Even after 30 min of reaction, the average thickness of the Al_3Ni_2 was approximately 2.1 μm, which is still a reasonable thickness for interfacial IMC layers [31]. It is widely known that excessive growth of IMCs has a tendency to cause the mechanical reliability of solder joints to deteriorate. Therefore, this slow growth rate of Al_3Ni_2 is regarded as beneficial for the reliability of solder joints.

The overall growth rate coefficient for all Cu-Zn IMCs was 2.18 $\mu m/s^{1/2}$, nearly 44 times higher than that for the Al_3Ni_2 in the Zn-5Al/Ni-W-P/Cu interconnects. Regarding the individual Cu-Zn IMCs, the growth rate coefficients (k) of γ-Cu_5Zn_8 and ε-$CuZn_4$ were 1.573 $\mu m/s^{1/2}$ and 0.551 $\mu m/s^{1/2}$, respectively, whereas the k value for the β-CuZn interlayer was the smallest at only 5.607×10^{-2} $\mu m/s^{1/2}$.

3.4. Diffusional formation mechanism of IMCs in Zn-Al solder interconnects

Based on the results discussed above, Fig. 7 schematically illustrates the diffusional formation mechanisms of the interfacial IMCs at Zn-Al solder interconnects. During the liquid-solid reactions at the Zn-Al/Cu interfaces, the Zn-5Al solder was in a liquidus state while the Cu remained solid. Zn atoms were abundant because of the fast diffusion rate in liquid. As a result, $CuZn_4$, a Zn-enriched phase, formed first. The mutual diffusion and reaction of these two elements were driven by the differences in concentration between the solder and the substrate matrix. By virtue of the high diffusion rates of Cu and Zn atoms in $CuZn_4$ layers, as reported by Gancarz and Xiao et al. [22,30], Cu_5Zn_8 could rapidly grow to form into the thickest layer among the various Cu-Zn IMC layers. The faster diffusion rate of the Zn element also triggered a vacancy flux in the opposite direction, generating vacancies in the $CuZn_4$ near the Cu_5Zn_8 phase. Then, these vacancies accumulated to form Kirkendall voids, as illustrated in Fig. 7 a). A similar phenomenon also occurs in Zn-Sn-Cu-Bi/Cu solder joints after 90 s of liquid reaction [24]. Afterwards, Zn atoms in the Cu_5Zn_8 phase slowly reacted with Cu atoms from the substrate to form a CuZn phase as the liquid-solid reaction continued. Thus, the enormous difference in the growth rates of the Cu_5Zn_8 and CuZn phases contributed to the unbalanced interdiffusion of the Cu and Zn elements. Consequently, the formation of Kirkendall voids near the CuZn layer is clearly unavoidable. This situation has seldom been previously reported in Zn-Al solder joints, but enormous efforts have been made with regard to conventional Sn-based solder joints, with similar findings concerning void formation in Cu_3Sn layers [12,25,26]. Based on these works, it can be predicted that these Kirkendall voids in Zn-Al solder joints could cause the mechanical reliability of Zn-Al solder joints to deteriorate. Overall, the interfacial reaction in a Zn-Al solder interconnect without a diffusion barrier is rather complex and accompanied by the formation of various defects, as illustrated in Fig. 7 a).

By contrast, when an electroless Ni-W-P coating was employed as a diffusion barrier, only Ni atoms diffused out from the metallisation and then reacted with Al atoms from the solder matrix to form a relatively thin Al_3Ni_2 layer (~2.15 μm after 30 min of reaction), according to the elemental analysis (see Fig. 5). The continuous growth of this thin Al_3Ni_2 IMC layer attracted Al and Ni atoms as they slowly diffused from the solder and the coating matrix, respectively. By preventing the formation of different types of IMCs, the formation of micro-sized Kirkendall voids near the Zn-5Al/Ni-W-P interface after liquid-solid reaction for up to 30 min could thus be avoided.

4. Conclusions

This study investigated the effects of electroless Ni-W-P coating as a diffusion barrier in high-temperature Zn-5Al solder joints. The interfacial reaction between the molten Zn-5Al solder and the electroless Ni-W-P coating was investigated, and Zn-5Al/Cu interconnects under the same reflow conditions were tested for comparison. The following conclusions can be drawn:

1. The presence of an electroless Ni-W-P coating can significantly decrease the thickness of the interfacial IMC layer that forms from 94 μm (Cu substrate, 30 min of reaction) to 2.15 μm (Ni-W-P-coated Cu substrate, 30 min of reaction), which demonstrates the excellent diffusion barrier property of electroless Ni-W-P coatings for preventing reactions between Zn-5Al solder and Cu.
2. At a Zn-5Al/Cu interface, three types of IMCs, namely, $CuZn_4$, Cu_5Zn_8 and CuZn, can be identified, and the overall growth rate coefficient for all IMCs is 2.18 $\mu m/s^{1/2}$. By contrast, when an electroless Ni-W-P coating is applied, the growth rate coefficient of the resulting Al_3Ni_2 layer is significantly lower (4.90×10^{-2} $\mu m/s^{1/2}$).
3. The interlayer at a Zn-5Al/Ni-W-P interface remains intact after liquid-solid reaction for a duration of 30 min. By contrast, a notable number of Kirkendall voids can be found at the

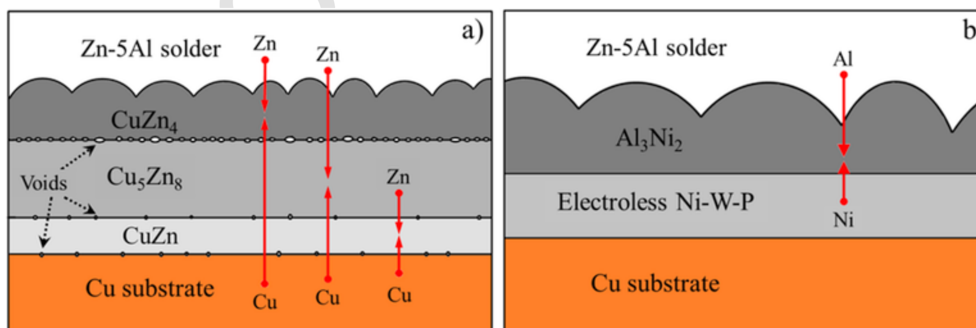

Fig. 7. Schematic diagrams illustrating the diffusional formation mechanisms at a) a Zn-5Al/Cu interface and b) a Zn-5Al/Ni-W-P interface.

CORRECTED PROOF

$CuZn_4/Cu_5Zn_8$, Cu_5Zn_8/CuZn and CuZn/Cu interfaces in Zn-5Al/Cu solder joints after prolonged reaction.

4. During liquid-solid reaction, the thickness of the IMC layer follows a parabolic law with respect to the reaction duration in both Zn-5Al/Cu and Zn-5Al/Ni-W-P/Cu interconnects. This finding indicates that the growth mechanism of the IMC layers is diffusion-controlled.

Acknowledgements

This research was supported by a Marie Curie International Research Staff Exchange Scheme Project within the 7th European Community Framework Programme, No. PIRSES-GA-2010-269113, entitled "Micro-Multi-Material Manufacture to Enable Multifunctional Miniaturised Devices (M6)", as well as an EPSRC-CPB Funding (GRANT NO. FS14). The authors also acknowledge the research funding by the National Nature Science Foundation of China (NSFC GRANT NO. 61261160498).

References

[1] S. Menon, E. George, M. Osterman, M. Pecht, High lead solder (over 85%) solder in the electronics industry: RoHS exemptions and alternatives, J. Mater. Sci. Mater. Electron. 26 (No. 6) (2015) 4021–4030.

[2] V.R. Manikam, K.Y. Cheong, Die attach materials for high temperature applications: a review, IEEE Trans. Compon. Packag. Manuf. Technol. 1 (No. 4) (2011) 457–478.

[3] Vivek Chidambaram, John Hald, Jesper Hattel, Development of Au–Ge based candidate alloys as an alternative to high-lead content solders, J. Alloys Compd. 490 (2010) 170–179.

[4] R. Koleňák, M. Chachula, Characteristics and properties of Bi-11Ag solder, Solder. Surf. Mt. Technol. 25 (No. 2) (2013) 68–75.

[5] T. Youssef, W. Rmili, E. Woirgard, S. Azzopardi, N. Vivet, et al., Power modules die attach: a comprehensive evolution of the nanosilver sintering physical properties versus its porosity, Microelectron. Reliab. 55 (No. 9–10) (2015) 1997–2002.

[6] M.S. Kim, H. Nishikawa, Effects of bonding temperature on microstructure, fracture behavior and joint strength of Ag nanoporous bonding for high temperature die attach, Mater. Sci. Eng. A 645 (2015) 264–272.

[7] A. Haque, B.H. Lim, A.S.M.A. Haseeb, H.H. Masjuki, Die attach properties of Zn–Al–Mg–Ga based high-temperature lead-free solder on Cu lead-frame, J. Mater. Sci. Mater. Electron. 23 (2012) 115–123.

[8] Tomasz Gancarz, Janusz Pstruś, Przemysław Fima, Sylwia Mosińska, Thermal properties and wetting behavior of high temperature Zn-Al-In solders, J. Mater. Eng. Perform. 21 (2012) 599–605.

[9] Yoshikazu Takaku, Lazuardi Felicia, Ikuo Ohnuma, Ryosuke Kainuma, Kiyohito Ishida, Interfacial reaction between Cu substrates and Zn-Al base high-temperature Pb-Free solders, J. Electron. Mater. 37 (2008) 314–323.

[10] Min He, Zhong Chen, Guojun Qi, Mechanical strength of thermally aged Sn-3.5Ag/Ni-P solder joints, Metall. Mater. Trans. A 36 (2005) 65–75.

[11] V. Vuorinen, T. Laurila, H. Yu, J.K. Kivilahti, Phase formation between lead-free Sn–Ag–Cu solder and Ni(P)/Au finishes, J. Appl. Phys. 99 (2006) 023530.

[12] K. Chen, C. Liu, D.C. Whalley, D.A. Hutt, J.F. Li, S.H. Mannan, A comparative study of the interfacial reaction between electroless Ni–P coatings and molten tin, Acta Mater. 56 (2008) 5668–5676.

[13] S.K. Tien, J.G. Duh, Y.I. Chen, Structure, thermal stability and mechanical properties of electroless Ni-P-W alloy coatings during cycle test, Surf. Coat. Technol. 177–178 (2004) 532–536.

[14] J.N. Balaraju, Kalavati, N.T. Manikandanath, V.K. William Grips, Phase transformation behavior of nanocrystalline Ni–W–P alloys containing various W and P contents, Surf. Coat. Technol. 206 (2012) 2682–2689.

[15] Dong Min Jang, Jin Yu, Tungsten alloying of the Ni(P) films and the reliability of Sn–3.5Ag/NiWP solder joints, J. Mater. Res. 26 (2011) 889–895.

[16] Ying Yang, J.N. Balaraju, Ser Choong Chong, Hui Xu, Changqing Liu, Vadim V. Silberschmidt, Zhong Chen, Significantly retarded interfacial reaction between an electroless Ni–W–P metallization and lead-free Sn–3.5Ag solder, J. Alloys Compd. 565 (2013) 11–16.

[17] K. Chen, C. Liu, D.C. Whalley, D.A. Hutt, Electroless Ni-W-P alloys as barrier coating s for liquid solder interconnects, In: 1st Electronics System Integration Technology Conference (ESTC), Dresden, Germany, 2006, pp. 421–427.

[18] Yoshikazu Takaku, Komei Makino, Keita Watanabe, Ikuo Ohnuma, Ryosuke Kainuma, Yasushi Yamada, Yuji Yagi, Ikuo Nakagawa, Takashi Atsumi, Kiyohito Ishida, Interfacial reaction between Zn-Al-Based high-temperature solders and Ni substrate, J. Electron. Mater. 38 (2009) 54–60.

[19] F.X. Che, John H.L. Pang, Characterization of IMC layer and its effect on thermomechanical fatigue life of Sn–3.8Ag–0.7Cu solder joints, J. Alloys Compd. 541 (2012) 6–13.

[20] W.H. Chen, C.F. Yu, H.C. Cheng, Y.M. Tsai, S.T. Lu, IMC growth reaction and its effects on solder joints thermal cycling reliability of 3D chip stacking packaging, Microelectron. Reliab. 53 (2013) 30–40.

[21] H.B. Qin, W.Y. Li, W.B. Zhou, X.P. Zhang, Low cycle fatigue performance of ball grid array structure Cu/Sn-3.0Ag-0.5Cu/Cu solder joints, Microelectron. Reliab. 54 (2014) 2911–2921.

[22] Tomasz Gancarz, Janusz Pstruś, Przemysław Fima, Sylwia Mosińska, Effect of Ag addition to Zn–12Al alloy on kinetics of growth of intermediate phases on Cu substrate, J. Alloys Compd. 582 (2014) 313–322.

[23] K. Suganuma, T. Murata, H. Noguchi, Y. Toyada, Heat resistance of Sn–9Zn solder/Cu interface with or without coating, J. Mater. Res. 15 (No.4) (2000) 884–891.

[24] Fei Xing, Jia Yao, Jingwei Liang, Xiaoming Qiu, Influence of intermetallic growth on the mechanical properties of Zn–Sn–Cu–Bi/Cu solder joints, J. Alloys Compd. 649 (2015) 1053–1059.

[25] Glenn Ross, Vesa Vuorinen, Mervi Paulasto-Kröckel, Void formation and its impact on Cu Sn intermetallic compound formation, J. Alloys Compd. 677 (2016) 127–138.

[26] Qingqian Li, Y.C. Chan, Growth kinetics of the Cu_3Sn phase and void formation of sub-micrometre solder layers in Sn–Cu binary and Cu–Sn–Cu sandwich structures, J. Alloys Compd. 567 (2013) 47–53.

[27] Cheng En Ho, Tsai Tung Kuo, Chun Chien Wang, Wei Hsiang Wu, Inhibiting the growth of Cu3Sn and Kirkendall voids in the Cu/Sn-Ag-Cu system by minor Pd alloying, Electron. Mater. Lett. 8 (2012) 495–501.

[28] K. Zeng, R. Stierman, T.C. Chiu, D. Edwards, K. Ano, K.N. Tu, Kirkendall void formation in eutectic SnPb solder joints on bare Cu and its effect on joint reliability, J. Appl. Phys. 97 (2005). 024508–1-8.

[29] Jin Yu, J.Y. Kim, Effects of residual S on Kirkendall void formation at Cu/Sn–3.5Ag solder joints, Acta Mater. 56 (2008) 5514–5523.

[30] Yong Xiao, Mingyu Li, Ling Wang, Shangyu Huang, Xueming Du, Zhiquan Liu, Interfacial reaction behavior and mechanical properties of ultrasonically brazed Cu/Zn–Al/Cu joints, Mater. Des. 73 (2015) 42–49.

[31] P. Xue, B.L. Xiao, D.R. Ni, Z.Y. Ma, Enhanced mechanical properties of friction stir welded dissimilar Al–Cu joint by intermetallic compounds, Mater. Sci. Eng. A 527 (2010) 5723–5727.

UNCORRECTED PROOF